X-ray-induced electronic structure change in $CuIr_2S_4$

H. Gretarsson,[1] Jungho Kim,[2] D. Casa,[2] T. Gog,[2] K. R. Choi,[3] S. W. Cheong,[3,4] and Young-June Kim[1,*]

[1]*Department of Physics, University of Toronto, 60 St. George Street, Toronto, Ontario M5S 1A7, Canada*

[2]*CMC-XOR, Advanced Photon Source, Argonne National Laboratory, Argonne, Illinois 60439, USA*

[3]*l_PEM, Pohang University of Science and Technology, Pohang 790-784, Korea*

[4]*R-CEM and Department of Physics and Astronomy, Rutgers University, Piscataway, New Jersey 08854, USA*

(Received 29 April 2011; revised manuscript received 2 September 2011; published 29 September 2011)

The electronic structure of $CuIr_2S_4$ is investigated using various bulk-sensitive x-ray spectroscopic methods near the Ir L_3 edge: resonant inelastic x-ray scattering (RIXS), x-ray absorption spectroscopy in the partial fluorescence yield mode, and resonant x-ray emission spectroscopy. A strong RIXS signal (0.75 eV) resulting from a charge-density-wave gap opening is observed below the metal-insulator transition temperature of 230 K. The resultant modification of electronic structure is consistent with the density functional theory prediction. In the spin- and charge-dimer disordered phase induced by x-ray irradiation below 50 K, we find that a broad peak around 0.4 eV appears in the RIXS spectrum.

DOI: 10.1103/PhysRevB.84.125135 PACS number(s): 71.30.+h, 61.80.Cb, 75.50.−y

I. INTRODUCTION

The role of relativistic spin-orbit interactions in condensed matter systems is drawing much attention recently, and there are intensive research efforts to elucidate the physics of materials with 5*d* electrons.[1–5] A thiospinel $CuIr_2S_4$ is such an example.[6,7] The high-temperature metallic phase has a cubic spinel structure,[8] but the system becomes insulating and diamagnetic with a triclinic structure below the metal-insulator transition (MIT) temperature of $T_{MI} \sim 230$ K.[9,10] The "A" site in the spinel structure is occupied by Cu, which is monovalent[11–13] and, therefore, inactive near the Fermi energy. Mixed-valent iridium ions ($Ir^{3.5+}$) occupy the B sites and form a pyrochlore lattice. From their powder neutron diffraction experiments, Radaelli and coworkers proposed an intriguing octamer model of charge ordering, in which Ir^{4+} ions form spin and structural dimers separated by nonmagnetic Ir^{3+} ions.[9] This unusual charge order (CO) was explained by Khomskii and Mizokawa as an orbitally driven Peierls transition. That is, a large overlap of Ir *d* orbitals along the (110)-type direction renders the band structure quasi-one-dimensional and susceptible to Peierls instability.[14]

What is mystifying is its behavior when the sample is irradiated with x rays or electrons. A significant drop in resistivity was observed when the sample was exposed to x-ray or electron irradiation at low temperatures ($T < 50$ K).[15,16] In addition, the resistivity change occurs quite slowly, over a period of several minutes, and this effect could be reversed by heating the sample above 100 K. Detailed single-crystal x-ray scattering studies showed that the long-range CO was destroyed and a short-range incommensurate CO appeared in this irradiation-induced low-temperature (IILT) phase.[17] Although spectroscopic data suggest that substantial electronic structure modification occurs at the MIT, no spectroscopic changes in this IILT phase below 50 K have been reported to date.[18,19] For example, opening of an insulating gap of 0.15 eV below the MIT temperature was observed in both optics[21] and photoemission experiments,[11,18] but the photoemission spectra did not show any change in the IILT phase.[18,19] X-ray spectroscopy provides a natural avenue for investigation of this intriguing behavior, since x rays can act as a radiation source as well as a probing particle. However, detailed investigation of electronic structure using core-level x-ray spectroscopy has been limited. Although several Ir 4*f* photoemission experiments have reported that Ir^{3+}/Ir^{4+} charge disproportion does exist in the insulating phase, due to its surface sensitivity, the interpretation has not been straightforward.[18–20] While x-ray absorption spectroscopy (XAS) at the S *K* edge has been valuable in detecting redistribution of S 3*p* states across the MIT,[12] Ir L_3-edge XAS has not been very useful due to broad spectral features arising from the short core-hole lifetime.[12,13] In this work, we report bulk-sensitive x-ray spectroscopic studies which allow us to obtain direct information regarding the Ir 5*d* electronic states across the MIT and also in the IILT phase. Utilizing resonant inelastic x-ray scattering (RIXS) and resonant x-ray emission spectroscopy (RXES), we observe that the Ir 5*d* t_{2g} band shifts as a result of the opening of an insulating gap in the CDW phase, which confirms density functional theory (DFT) calculations.[22,24,25] We also find that a midinfrared peak in the RIXS spectrum emerges around 0.4 eV in the IILT phase, suggesting that not only the crystal[17] but also the electronic structure is modified due to the x-ray irradiation. To explain this experimental observation, we propose a model in which local dimers freed from the long-range CO can hop around.

II. EXPERIMENTAL DETAILS

All x-ray measurements were carried out at the Advanced Photon Source on the undulator beamline 9ID-B. The beam was monochromatized by a double-crystal Si(111) and a Si(444) channel-cut secondary crystal. For the Ir L_3-edge RIXS a spherical (1-m-radius) diced Si(844) analyzer was used and an overall energy resolution of 0.15 eV (FWHM) was obtained. The incident photon polarization vector was rotated with a diamond phase plate to bring it parallel to the vertical scattering plane (π polarization). In this geometry, due to the polarization factor, the contribution from Thomson scattering is minimized. At this photon energy, the sample probing depth is more than 10 μm, allowing one to study the true bulk electronic properties. Most of the measurements were carried out near $\mathbf{Q} = (7\,7\,8)$ in order to keep 2θ close to 90°. We

also utilized a high-resolution setup with a Si(844) channel-cut secondary monochromator and a horizontal scattering geometry. In this setup no phase plate was needed to obtain π polarization. This provided an overall energy resolution of 0.08 eV (FWHM) and a significant reduction of the elastic line. For RXES and XAS in the partial fluorescence yield mode (PFY-XAS), a spherical (1-m-radius) diced Ge(337) analyzer was used to provide an overall energy resolution of 0.13 eV (FWHM). No diamond phase plate was used for these measurements. A single crystal of $CuIr_2S_4$ was grown by the bismuth solution method, as previously described in Ref. 17 and references therein. The crystal has a triangular shape, with the surface normal along the (111) direction. Throughout this paper, we use the cubic notation ($a = 9.8474$ Å) for simplicity.[8]

III. EXPERIMENTAL RESULTS

Wide energy range spectra obtained with all three experimental methods are shown in Fig. 1. In Fig. 1(a), the XAS spectrum near the Ir L_3 edge is shown as the dashed line, which was obtained by monitoring the total fluorescence yield. The PFY-XAS spectrum, shown as the solid line, is the incident energy dependence of the Lα_2 emission line ($3d_{3/2} \rightarrow 2p_{3/2}$) intensity. The benefit of the PFY mode is quite clear from this figure. By suppressing the spectral broadening due to the $2p$ core-hole lifetime,[26] sharper features are observed. The wide-range RXES and RIXS data are presented in the bottom panels in Fig. 1. In Fig. 1(b), the detailed evolution of the Lα_2 emission line as a function of incident energy (E_i) and emitted energy (E_f) is shown. In Fig. 1(c), a RIXS intensity map is plotted as a function of E_i and energy loss ($\hbar\omega \equiv E_i - E_f$).

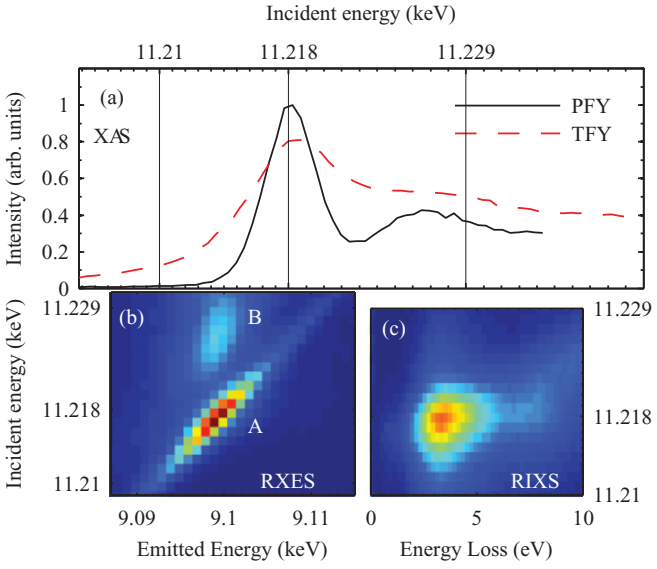

FIG. 1. (Color online) (a) Ir L_3-edge PFY-XAS taken by monitoring the intensity of Lα_2 ($3d_{3/2} \rightarrow 2p_{3/2}$) as a function of the incident energy. Included is the normal XAS obtained by monitoring the total fluorescence yield (TFY). (b, c) Wide range intensity map of both RXES and RIXS spectra as a function of the incident energy. Measurements were carried out at $\mathbf{Q} = (6.3\ 7\ 8.3)$ in the insulating phase ($T = 220$ K).

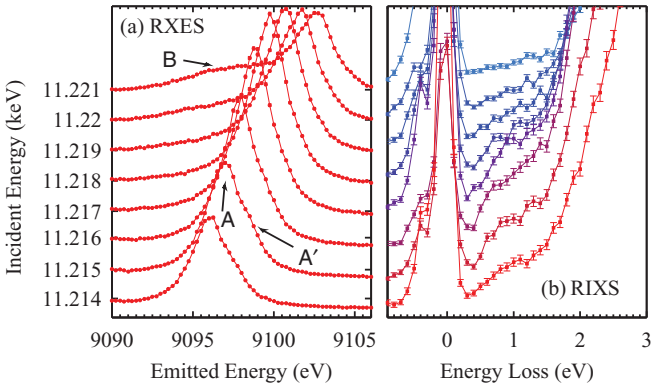

FIG. 2. (Color online) (a) Incident energy dependence of RXES spectra taken at $T = 250K$. (b) Incident energy dependence RIXS spectra taken at $T = 220$ K and with $\mathbf{Q} = (6.3\ 7\ 8.3)$. Data were taken with an incident photon energy of $11.214\ \text{keV} \leqslant E_i \leqslant 11.221$ keV. The spectra have been shifted to match the scale on the left.

The RXES data in Fig. 1(b) show two distinct features. There is a broad, strong feature (A) with a maximum intensity around $E_i = 11.218$ keV and another feature (B) that resonates at a higher incident energy. While feature B shows normal fluorescence behavior with fixed energy emission, the emitted photon energy of feature A shifts with E_i. This indicates that feature A comes from exciting an Ir $2p$ electron into an unoccupied *bound* state and thus the outgoing photon has a fixed energy loss. In this so-called Raman regime the RXES spectra can be understood as the unoccupied density of states, resonantly enhanced over the core-hole width.[27] Feature A then corresponds to empty Ir $5d$ e_g states. The evolution of feature A as a function of E_i at $T = 250$ K is shown in Fig. 2(a). On the high-energy side of A there is a prominent shoulder, A′, which can be associated with empty t_{2g} states. Note that the A′ feature is resonantly enhanced for E_i, which is 2–3 eV below the resonance of feature A. The intensity ratio can be explained by the fact that there are more empty e_g states than t_{2g} states (naively, 4 e_g states and 0.5 t_{2g} states). This intensity ratio, in addition to the $2p$ core-hole broadening, is why the t_{2g} state has not been revealed in previous XAS studies[12,13] and, in fact, was not observed in our PFY-XAS. Only by utilizing the resonance enhancement of RXES can one see this state.

Figure 3(a) shows the Lα_2 RXES spectra taken at $E_i = 11.215$ keV below and above the MIT. In the metallic phase, the Lα_2 emission line clearly has two components, A and A′, while only A is seen in the insulating phase. The Lα_2 emission line at $T = 250$ K has been fitted with two Voigt functions, representing A and A′. The separation of the two peaks is estimated from the fit to be $\Delta E_{AA'} \approx 1.65$ eV[28]. As we go below the MIT ($T = 215$ K) the emission line appears as a single peak A; nevertheless, we could extract A′ by fitting the same two-peak Voigt functions used for the ($T = 250$ K) case, with only their positions varied (amplitudes and widths were fixed). Here we have assumed that the instrumental resolution and lifetime broadening are constant across the MIT. The result shows almost no shift for A but the A′ feature shifts significantly, by $\Delta E \approx 0.55$ eV. This observation can be consistently explained by the DFT calculation result, which is

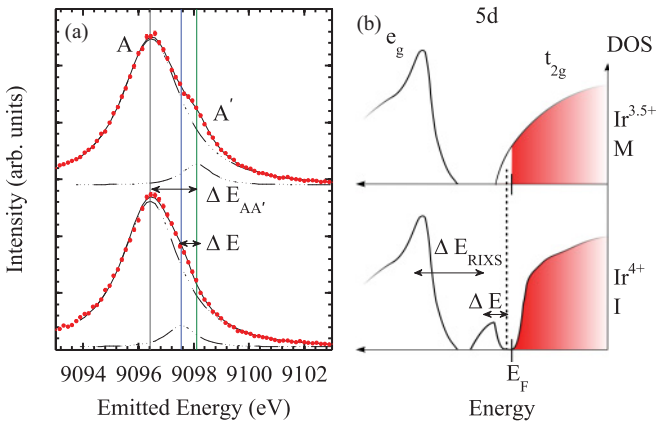

FIG. 3. (Color online) (a) Lα_2 RXES taken above and below the MIT at $E_i = 11.215$ keV. Dashed curves are the result of a fit (see text). ΔE represents the shift of A′. (b) Schematic diagram of the DOS below (I) and above (M) the MIT inferred from our experiment. ΔE_{RIXS} represents the splitting seen in RIXS.

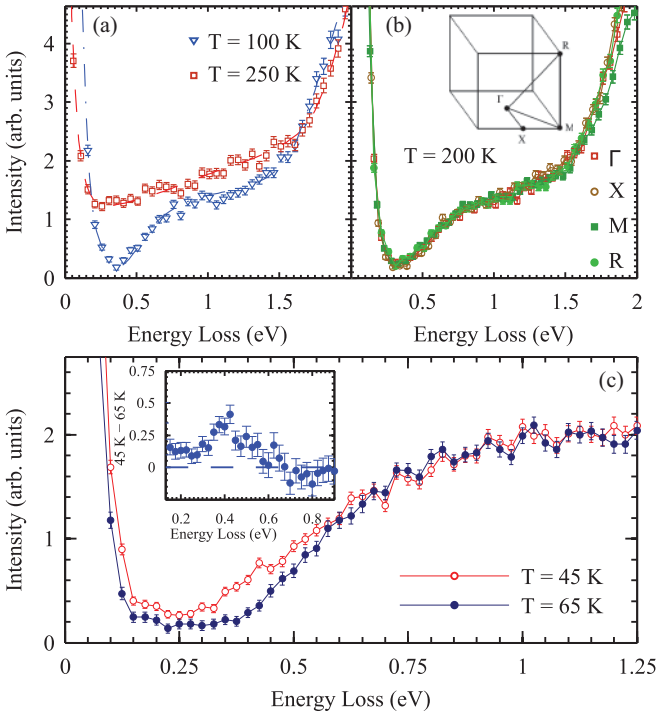

FIG. 4. (Color online) (a) Temperature dependence of the RIXS signal taken at $\mathbf{Q} = (6.15\ 7\ 8.5)$ for $E_i = 11.216$ keV. (b) Momentum dependence as measured at the high-symmetry positions indicated in the inset. (c) High-resolution RIXS spectra taken above ($T = 65$ K) and within ($T = 45$ K) the charge-disordered phase. To emphasize the difference induced by irradiation we show the subtracted spectra in the inset.

schematically shown in Fig. 3(b).[22,25] The main observation in our RXES study is that the opening of an insulating gap occurs due to a shift of the empty t_{2g} band with respect to the empty e_g band.

In Fig. 1(c), a broad and strong RIXS feature in the 2- to 6-eV range can be seen, which shows a large resonant enhancement near $E_i = 11.218$ keV. The weak higher energy (7–9 eV) feature is a fluorescence line. In between these high-energy excitations and the elastic peak ($\hbar\omega = 0$), we observe a sharp edge-like RIXS feature around $\hbar\omega \approx 0.75$ eV, which is clearly seen in the individual scans shown in Fig. 2(b). This feature seems to resonate at about 2 eV below the resonance energy of the 2- to 6-eV feature. This resonance behavior is crucial in identifying the observed spectral features. As in the interpretation of the RXES data, the intermediate states accessed through the main absorption feature at $E_i = 11.218$ keV are the Ir 5d e_g levels, and therefore the 2- to 6-eV excitation can be naturally associated with a transition into empty bands of hybridized Ir 5d e_g and S 3p character.[11,25] The 0.75-eV feature, resonating around 11.216 keV, can then be identified as the d-d transition into an empty t_{2g} state. The energy difference between these two excitations represents the splitting between the empty e_g and t_{2g} states and is found to be about 2.8 eV. This splitting is also consistent with the DFT and cluster model calculation value of about 2.6 eV.[22,23]

In Fig. 4(a) we show in detail the temperature dependence of the low-energy RIXS spectrum. The temperature dependence shows a drastic spectral change as the sample goes through the MIT. In the metallic phase at $T = 250$ K, a nonzero intensity is observed at low energies. Once we go through the MIT a gap opens around 0.3 eV in the RIXS spectrum indicating the insulating state, which is consistent with the optical study.[21] According to the DFT calculation, in the high-temperature metallic phase, hybridized Ir t_{2g} and S 3p bands cross the Fermi level,[22] giving rise to the low-energy spectral weight observed below the gap. Below $T = 230$ K, an insulating gap opens in this band. The difference in the absolute level of the spectral weight above the gap is probably due to the difference in resonance condition, since electronic structure changes quite dramatically across the MIT. The momentum dependence of the insulating gap is shown in Fig. 4(b). It was taken along high-symmetry directions as shown in the inset, where Γ is $\mathbf{Q} = (7\ 7\ 8)$. Scans at the high-symmetry positions, shown in Fig. 4(b), exhibit no $\mathbf{q}$ dependence. This indicates that the gap opening is more or less uniform in reciprocal space, suggesting that the band width of the empty t_{2g} band is fairly narrow. We have also measured the temperature and momentum dependence of the 2- to 6-eV feature (not shown), but no significant changes were seen.

When the sample was cooled below $T = 50$ K while irradiated with x rays, a sudden drop in resistivity was observed.[15,16] It was found that not only x rays, but also electron, visible light, and even high-energy ion beams, could induce this IILT phase.[15,17,18,29] We have obtained high-resolution RIXS data in this phase, shown in Fig. 4(c), by cooling the system with x rays impinging on the sample. A considerable increase in the spectral weight below 0.6–0.7 eV was observed. By subtracting the $T = 65$ K spectrum from the $T = 45$ K one, we can see that this intensity comes from the peak formed around 0.4 eV (shown in the inset) rather than from the tail of the elastic peak. The spectrum does not resemble the one at $T = 300$ K either, which indicates that the IILT phase is different from the original high-temperature metallic phase, in agreement with structural studies.[17,30,31] We also measured the Lα_2 RXES spectra for $T < 50$ K, but no difference was observed. We note that the larger elastic

intensity ($\hbar\omega \lesssim 0.15$ eV) at $T = 45$ K compared to $T = 65$ K is due to the increased diffuse scattering when the long-range CO is lost.[17]

IV. DISCUSSION

Even when the long-range CO is destroyed, it is known that individual dimers do exist in this phase.[30] One can imagine that when there is no long-range order, dimers can hop around more easily, and the increased hopping rate of dimers could be responsible for the decreased resistivity in this phase. In fact such dynamic dimers could be responsible for the midinfrared peak seen around 0.4 eV, which is reminiscent of the polaron peak observed in manganites.[32] Since dimers of Ir^{4+}-Ir^{4+} have significantly smaller bond lengths than Ir^{3+}-Ir^{3+}, they will introduce lattice distortion as well as CO defects in the crystal, as they move around incoherently. Such an incoherent motion of dimers could be strongly coupled to the lattice, resulting in the formation of a bipolaron-like object. Further high-resolution spectroscopic study of this x-ray-induced phase, such as optical conductivity, could shed light on this possibility.

In summary, we report comprehensive bulk-sensitive x-ray spectroscopy studies of electronic structure in $CuIr_2S_4$. We show that the Ir 5d t_{2g} band shifts as a result of the opening of a charge-density-wave gap, which is consistent with band theory calculations. In the low-temperature x-ray induced phase, we found that a broad peak around 0.4 eV appears in the RIXS spectrum, which could arise from the dynamic hopping of local dimers.

ACKNOWLEDGMENTS

We would like to thank Y. B. Kim, N. Perkins, and H. Takagi for valuable discussions. Research at the University of Toronto was supported by the NSERC of Canada, Canadian Foundation for Innovation, and Ontario Ministry of Research and Innovation. Use of the Advanced Photon Source was supported by the U.S. DOE, Office of Science, Office of Basic Energy Sciences, under Contract No. W-31-109-ENG-38.

*yjkim@physics.utoronto.ca

[1] Y. Okamoto, M. Nohara, H. Aruga-Katori, and H. Takagi, Phys. Rev. Lett. **99**, 137207 (2007).
[2] B. J. Kim *et al.*, Phys. Rev. Lett. **101**, 076402 (2008).
[3] G. Jackeli and G. Khaliullin, Phys. Rev. Lett. **102**, 017205 (2009).
[4] A. Shitade, H. Katsura, J. Kunes, X. L. Qi, S. C. Zhang, and N. Nagaosa, Phys. Rev. Lett. **102**, 256403 (2009).
[5] D. Pesin and L. Balents, Nature Phys. **6**, 376 (2010).
[6] S. Nagata, T. Hagino, Y. Seki, and T. Bitoh, Physica B **194**, 1077 (1994).
[7] S. Nagata, N. Matsumoto, Y. Kato, T. Furubayashi, T. Matsumoto, J. P. Sanchez, and P. Vulliet, Phys. Rev. B **58**, 6844 (1998).
[8] T. Furubayashi *et al.*, J. Phys. Soc. Jpn. **63**, 3333 (1994).
[9] P. G. Radaelli *et al.*, Nature (London) **416**, 155 (2002).
[10] H. Ishibashi, T. Sakai, and K. Nakahigashi, J. Magn. Magn. Mater. **226–230**, 233 (2001).
[11] J. Matsuno, T. Mizokawa, A. Fujimori, D. A. Zatsepin, V. R. Galakhov, E. Z. Kurmaev, Y. Kato, and S. Nagata, Phys. Rev. B **55**, R15979 (1997).
[12] M. Croft, W. Caliebe, H. Woo, T. Tyson, D. Sills, Y. S. Hor, S. W. Cheong, V. Kirykukhin, and S. J. Oh, Phys. Rev. B **67**, 201102 (2003).
[13] N. Kijima *et al.*, J. Alloys Compd. **480**, 120 (2009).
[14] D. I. Khomskii and T. Mizokawa, Phys. Rev. Lett. **94**, 156402 (2005).
[15] H. Ishibashi, T. Y. Koo, Y. S. Hor, A. Borissov, P. G. Radaelli, S. W. Cheong, and V. Kiryukhin, Phys. Rev. B **66**, 144424 (2002).
[16] T. Furubayashi *et al.*, Solid State Commun. **126**, 617 (2003).
[17] V. Kiryukhin, Y. Horibe, Y. S. Hor, M. J. Noh, S. W. Cheong, and C. H. Chen, Phys. Rev. Lett. **97**, 225503 (2006).
[18] K. Takubo, S. Hirata, J.-Y. Son, J. W. Quilty, T. Mizokawa, N. Matsumoto, and S. Nagata, Phys. Rev. Lett. **95**, 246401 (2005).
[19] K. Takubo, T. Mizokawa, N. Matsumoto, and S. Nagata, Phys. Rev. B **78**, 245117 (2008).
[20] H.-J. Noh, E. J. Cho, H. D. Kim, J. Y. Kim, C. H. Min, B. G. Park, and S. W. Cheong, Phys. Rev. B **76**, 233106 (2007).
[21] N. L. Wang, G. H. Cao, P. Zheng, G. Li, Z. Fang, T. Xiang, H. Kitazawa, and T. Matsumoto, Phys. Rev. B **69**, 153104 (2004).
[22] T. Oda *et al.*, J. Phys. Condens. Matter **7**, 4433 (1995).
[23] K. Kitamoto, Y. Taguchi, K. Mimura, K. Ichikawa, O. Aita, and H. Ishibashi, Phys. Rev. B **68**, 195124 (2003).
[24] T. Sasaki *et al.*, J. Phys. Soc. Jpn. **73**, 1875 (2004).
[25] S. Sarkar, M. De Raychaudhury, and T. Saha-Dasgupta, Phys. Rev. B **79**, 113104 (2009).
[26] K. Hämäläinen, D. P. Siddons, J. B. Hastings, and L. E. Berman, Phys. Rev. Lett. **67**, 2850 (1991).
[27] M. H. Krisch, C. C. Kao, F. Sette, W. A. Caliebe, K. Hamalainen, and J. B. Hastings, Phys. Rev. Lett. **74**, 4931 (1995).
[28] The value of $\Delta E_{AA'}$ is much smaller than the e_g-t_{2g} splitting of 2.8 eV observed through RIXS. This difference is the RXES final-state effect, since the 3*d* core hole interacts with the open 5*d* shell [S. Nakai *et al.*, J. Electron Spectrosc. Relat. Phenom. **137**, 363 (2004)]. However, the relative shift of A′ with respect to A is not affected by the final-state effect.
[29] M. Koshimizu, H. Tsukahara, and K. Asai, Nucl. Instrum. Methods Phys. Res. Sec. B **267**, 1125 (2009).
[30] E. S. Božin, A. S. Masadeh, Y. S. Hor, J. F. Mitchell, and S. J. L. Billinge, Phys. Rev. Lett. **106**, 045501 (2011).
[31] W. Sun *et al.*, J. Phys. Soc. Jpn. **70**, 2817 (2001).
[32] K. H. Kim, J. H. Jung, and T. W. Noh, Phys. Rev. Lett. **81**, 1517 (1998).